Three-Dimensional Structure Formation of Polypropylene Revealed by in Situ Scanning Force Microscopy and Nanotomography

Mechthild Franke and Nicolaus Rehse*

Chemische Physik, TU Chemnitz, 09107 Chemnitz, Germany

Received August 17, 2007; Revised Manuscript Received October 12, 2007

ABSTRACT: A detailed model for the three-dimensional growth of a screw dislocation and a γ-branching of a lamella of elastomeric polypropylene (ePP) is proposed. The crystallization of a thin film was followed with in situ scanning force microscopy (SFM). Nucleation and growth of individual defects were observed with high temporal and spatial resolution. To identify the three-dimensional volume structure, the defects were examined with nanotomography, which is a layer-by-layer imaging technique based on SFM.

Introduction

Polypropylene is increasingly applied in industrial products because of its tunable mechanical properties.[1] These properties can be mainly ascribed to the microstructure of the polymer, which consists of small crystalline entities embedded in an amorphous matrix. Therefore, much research has been done to study the crystallization in situ by using different methods such as small-angle X-ray scattering[2,3] and wide-angle X-ray scattering.[4,5] However, these methods give only information on the average volume structure of the material. To study the real space structure, many in situ experiments concerning the crystal growth were done with the help of scanning force microscopy.[6−14] This technique led to new insights into crystallization and melting processes, e.g., the influence of helix conformation in isotactic polypropylene as shown by Zhou et al.[6] or the melting of unstable nuclei as shown by Schönherr et al.[7] Although SFM is a rather straightforward experiment, one has to be aware of the influence of the scanning tip.[8] Because this method is restricted to the surface of the sample, insights into the volume microstructure forming process could not be provided, e.g., while the observation of the growth of a screw dislocation is rather obvious,[6] it is not possible to distinguish between a screw dislocation and a breaking of a lamella from side view.

Recently we have used nanotomography[15] to reveal the three-dimensional microstructure of an elastomeric isotactic polypropylene (ePP) sample.[16] We could identify orientation and shape of individual crystals as well as their connectivity. Another emerging technique to observe the three-dimensional morphology is transmission electron microtomography (TEMT),[17] which was also used to investigate semicrystalline polymers.[18] Here the authors were able to image polymer crystals with a very high resolution.

In this paper we have studied the crystallization process of ePP with in situ tapping mode SFM in real space. The used polymer is similar to the ePP used in refs 7 and 16. It has a very low tacticity, resulting in a low crystallinity. After crystallization nanotomography is applied to exactly the same area observed before. Following the structure formation during the crystallization and subsequently imaging the three-dimensional microstructure of the same area with nanotomography leads to new information on the crystallization especially on the formation of individual defects.

* Corresponding author. E-mail: nicolaus.rehse@physik.tu-chemnitz.de.

Experimental Section

We study ePP with a weight-average molecular weight M_w of 110 kg/mol and a [*mmmm*]-pentad content of 28% synthesized by metallocene catalyzed polymerization.[19] Polymer films ($\sim$ 1 μm thick) on gold coated silicon were prepared by dip-coating from a 0.5 wt % ePP solution in decaline.

After drying the films in air, the films were melt at 175 °C under nitrogen atmosphere for about 20 min and subsequently quenched to room temperature, transferred into the SFM (MultiMode SFM with NanoScope III controller, Digital Instruments, Santa Barbara, CA), and the observation was started immediately using tapping mode. Height and phase images were recorded simultaneously at a rate of 3 min per image. Silicon tips with a spring constant of $\sim$ 40 N/m and a resonance frequency of $\sim$ 300 kHz were used. To reduce the influence of the scanning tip on the sample a high amplitude ratio $A_{ts}/A_0 = 0.85$ was used. To correct for drift a home-built offset tool was used.[20]

We have stopped the observation when no further changes were obvious. Nanotomography was applied to the same area observed before. The layer-by-layer removal was done by wet chemical etching as described in ref 16. The resulting 42 layers were processed as described in refs 16 and 21. The images were stacked by a mutual distance of 6 nm corresponding to the averaged etching rate.[16] A median filter with a 3 × 3 kernel was applied in $x-z$- and $y-z$-directions to remove artifacts of the etching process which appear only in one layer.

Results and Discussion

Crystallization. Figure 1 shows tapping mode SFM phase images of the observed area $\sim$ 20 and 230 min after quenching (see also Supporting Information).

Bright areas correspond to lamellae and dark areas to the amorphous phase. Because of the influence of the interfaces in the thin film the crystallites grow in edge-on configuration, therefore, they appear as bright lines. A scale bar for the phase shift values is not shown, since only relative values are needed to discriminate the two materials. The bright spots surrounded by dark regions (arrow in Figure 1a), which do not change with time, are probably features of the silicon substrate. It is interesting to note that nucleation does not happen at these features.

We find different morphologies of crystallites. Some lamellae grow without branching for a long time (A in Figure 1a), others branch a lot and build up bundles of lamellae (B in Figure 1a), which were described as "flower like" by Schönherr et al.[7] Finally, some lamellae show only a few, more separate branches (C in Figure 1a). The latter branches usually appear under an

10.1021/ma0718649 CCC: $40.75
Published on Web 12/11/2007

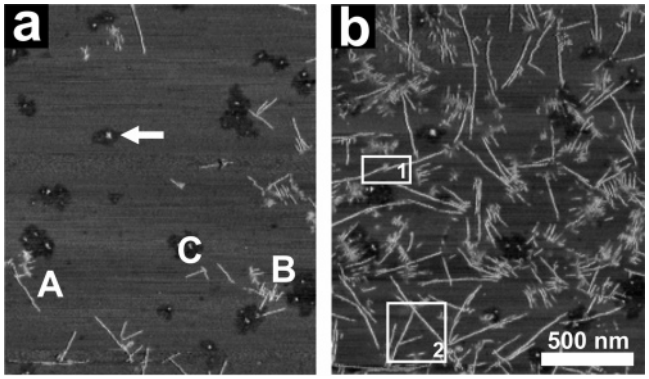

Figure 1. SFM phase images of the crystallization process showing an overview of the lamellar evolution. (a) 16 min after quenching; (b) 230 min after quenching. Bright areas correspond to hard crystalline material; dark areas correspond to soft amorphous material. Different morphologies of lamellae are found; without branching (A) or bundles of lamellae (B) as well as lamellae with single branches (C). Bright spots surrounded by dark areas do not change with time and can therefore be used as markers to correct for thermal drift. The full image sequence can be found in the Supporting Information.

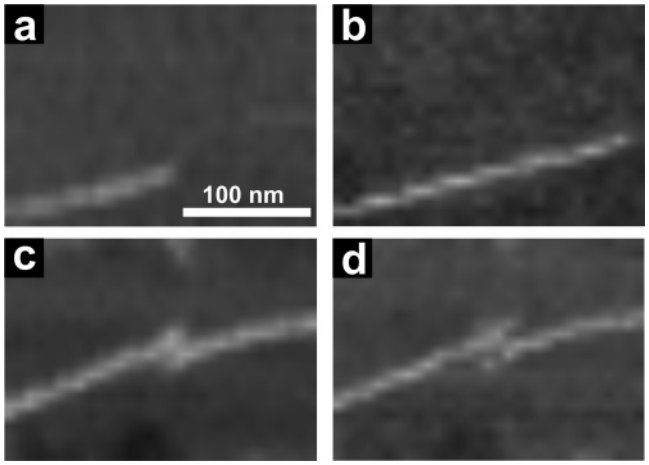

Figure 2. SFM phase images of a growing lamella (boxed area 1 in Figure 1b). (a) 55 min, (b) 73 min, (c) 169 min, and (d) 190 min after quenching. The full image sequence can be found in the Supporting Information.

angle of ~80°, which is typical for the α-form of isotactic polypropylene (iPP). This shows that the general crystallization in a low tacticity polymer, as used here, is similar to crystallization in high tacticity polypropylene.[14]

First lamellae appear ~10 min after quenching the sample to room temperature. Not all lamellae appear at the same time, as can be seen in comparison of Figure 1a and Figure 1b. In Figure 1a some lamellae are already nucleated and grow, while in areas covered by lamellae in Figure 1b, is still amorphous material in Figure 1a, which means that lamellae in these regions formed later. Also the growth of individual lamellae does not end at the same time. Some lamellae are still growing, while others already stopped. We have found no disintegration of small nuclei as reported in refs 12 and 7. A possible reason could be the higher crystallization temperature (41 °C) or the different polymer (polyether) investigated, respectively.

Figure 2 shows a sequence of images at the position of the boxed area 1 in Figure 1b (see also Supporting Information).

It shows a lamella, which grows continuously in the beginning of the observation (Figure 2a,b). After 1.5 h, the lamella appears to thicken at one spot (Figure 2c). At the end of measurement we observe two separate lamellae with parallel orientation (Figure 2d), however, shifted by an offset of approximately twice

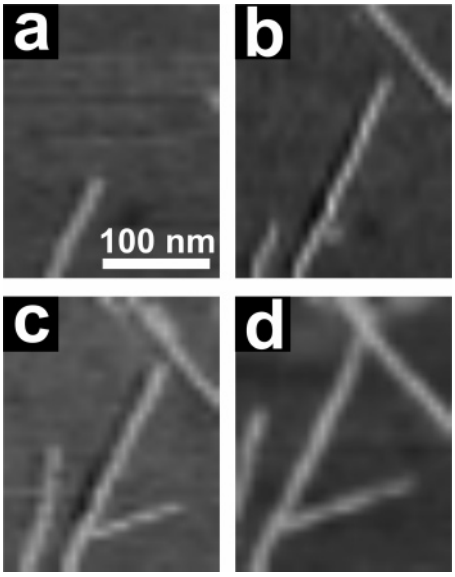

Figure 3. SFM phase images of a growing lamella (boxed area 2 in Figure 1b). (a) 16 min, (b) 37 min, (c) 75 min, and (d) 264 min after quenching. The full image sequence can be found in the Supporting Information.

the lamella thickness. Watching the whole sequence of phase images (Supporting Information) the lamella appears to be split into two parts. The same behavior was also found in other areas of Figure 1.

Figure 3 shows another sequence of images of the boxed area 2 in Figure 1b (see also Supporting Information).

Figure 3a shows a single growing lamella without any branches. Further growth of this mother lamella is hindered by an already existing lamella which lies in the growth direction (Figure 3b). In this image, we also observe a branching nucleus that has formed on the lamella. This nucleus then develops into a daughter lamella (Figure 3c,d). The angle between mother and daughter lamella is about 43°. We note that the angle does not change during crystallization. This angle is typical for the rather rare γ-morphology of iPP.[22,23]

Nanotomography. As described above, we have followed two phenomena, the splitting and the branching of a lamella with high temporal and spatial resolution. By considering only these information accessible from the surface of the film, it is not possible to explain the details of the crystallization process of these individual phenomena. To reveal the three-dimensional shape and orientation of the lamellae we have applied nanotomography to the same area observed in the crystallization experiment done before.

Figure 4 shows the nanotomography data of the lamella shown in Figure 2.

In Figure 4a, the isosurface of the lamella is displayed, i.e., the surface including all data points with a given threshold of the tapping mode phase value. The threshold was chosen in such way that the amorphous phase appears transparent. Figure 4b−e are phase images before etching and after 3, 6, and 9 etching steps, respectively. Neighboring crystallites are not shown for clarity. These images correspond to sections indicated in Figure 4a.

From Figure 4a, it is obvious that the lamella is not perpendicular to the surface. Also the lamella is not totally straight but is slightly curved. In the upper part, the lamella shows a bulge. At the surface the lamella seems to be separated and the two parts are parallel to each other (Figure 4b). Nanotomography reveals that at a depth of 18 nm the lamella

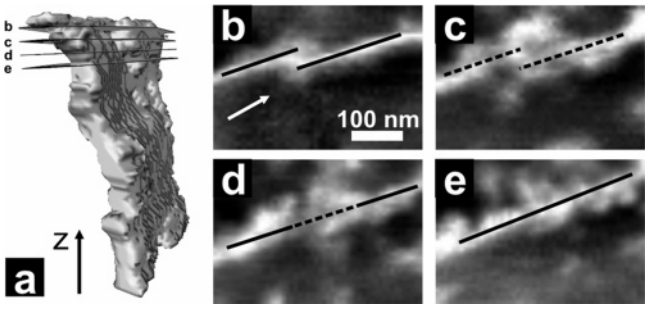

Figure 4. Nanotomography data (boxed area 1 in Figure 1b). (a) Isosurface containing all phase values with a chosen threshold (54%). (b) SFM phase images before etching. Images after (c) three, (d) six, and (e) nine etching steps. Parts b−e correspond to the sections indicated in the isosurface visualization (a). The lines in parts b−e indicate the lamella(e). The arrow in Figure 4b indicates the viewing direction for Figure 4a.

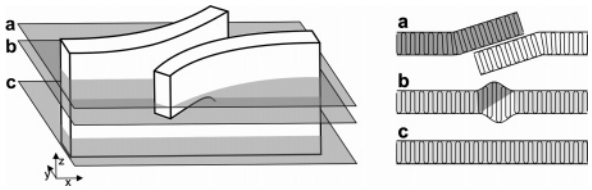

Figure 5. Schematic drawing of a screw dislocation (left). Right: top view of the sections labeled a, b, and c in the left drawing.

appears grainy (Figure 4c). The area, in which the splitting was observed, is smeared out. As a guide for the eye the dotted lines indicate the position of the lamella in Figure 4b. After further etching the shift between the two parts of the lamella decreases (Figure 4d) until they finally merge into one single lamella (Figure 4e).

Considering the observation during the crystal growth and the facts from the nanotomography the explanation for the splitting of the lamella is a screw dislocation as shown in Figure 5.

On the left side a three-dimensional sketch of the observed lamella is shown. The sections (a, b, and c) through the lamella are displayed on the right. Note that the molecular orientation is only indicated and should not be taken as real or measured.

In both, crystallization process and nanotomography data, the lamella appears continuous at one time or depth, respectively. And in both cases the lamella splits up at a certain time or depth. This indicates that a certain time in the crystallization experiment corresponds to a depth in the nanotomography experiment. Therefore, the lamella does not only grow laterally but also grows in the *z*-direction. In the crystallization experiment we first observe a continuous lamella (Figure 2a,b). This corresponds to sections e and c through the lamella in Figure 4 and 5, respectively. During the growth a thickening and misalignment was observed (Figure 2c). This corresponds to sections c and d in Figure 4 and section b in Figure 5. Finally, we observe two individual, parallel lamellae, which can also be seen in the nanotomography data (Figure 4b) and in the section a in Figure 5. Summarizing the first observation, we could ascribe the splitting to a screw dislocation as described by Bassett.[24]

Nanotomography slices of the area of Figure 3 in depths of 0 (a), 36 (b), and 54 nm (c) and sections perpendicular to the surface (d−f) are displayed in Figure 6.

At the surface the marked angle between the two lamellae is about 43° (Figure 6a). This is the same angle as observed during the crystallization. However, with increasing depth this angle is decreasing (Figure 6b,c) and the daughter lamella vanishes at a depth of ∼100 nm. This can be even better observed in a cross section where the distance between the two lamellae decreases with increasing depth (Figure 6d). A cross section some nanometers away from the branching point shows that the two lamellae are parallel and separated by a 20 nm wide amorphous region (Figure 6e). However, at the branching point we find no amorphous region between the mother and the daughter lamella (Figure 6f). To sum up the mother lamella has a rather straight shape whereas the daughter lamella is twisted. We note that the length of the daughter lamella does not change significantly with depth. Therefore, it is not possible to identify a nucleus assuming a radial growth of the daughter lamella. We have observed that the mother lamella was already formed as the daughter (twisted) lamella was nucleated. As a result most of the crystallizable parts of chains were already included into the mother lamella, and only a few were left, leading to a depletion zone around the mother lamella. We also find that the daughter lamella was nucleated in parallel orientation to the mother lamella as described in ref 25. Because of the depletion zone it grew away from the mother lamella. However, the angle between the mother and the daughter lamella increases with decreasing etching depth which could be explained by a twisted growth of the daughter lamella. Close to the surface the angle reaches a value of ∼43°, which is typical for the γ-branching from an α-lamella in defect rich iPP. This might be a favorable arrangement since it allows for an epitaxial growth of the daughter lamella. The γ-branching would also explain that we find no amorphous region where the two lamellae coincide (Figure 6f). Figure 6g shows a scheme of the straight mother and twisted daughter lamella. The lamellar growth in time and depth is indicated by the arrows labeled

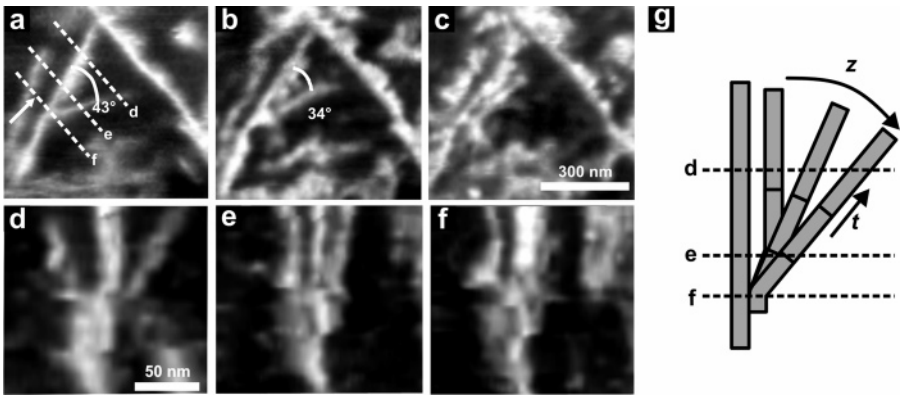

Figure 6. SFM phase images (enlargement of the boxed area 2 in Figure 1b) before and after etching, corresponding to a depth of 0, 36, and 66 nm in parts a−c, respectively. (d−f) Sections perpendicular to the surface at the positions indicated in part a. The arrow indicates the line of sight. (g) Growth scheme of the daughter lamella.

t and z, respectively. This second example shows that the combination of in situ real space crystallization experiments and nanotomography leads to novel insights into the crystallization process of ePP.

Conclusion

We have made some interesting observations during the crystal growth of ePP. These observations were further investigated using nanotomography. By using both, the information from the SFM image sequence and the volume image from the nanotomography experiment, we were able to explain crystallization phenomena in more detail than by using only one technique. The unusual splitting of an existing lamella could be ascribed to the formation of a screw dislocation. We could show that the more common branching of a lamella is a much more complex phenomenon when the third dimension comes into play. We note that both observations in the 2D-crystallization experiment might have been interpreted in a different way and only the combination with nanotomography gives the comprehensive view.

In the future new developments in automation of nanotomography[20] which allow for faster volume image acquisition and new fast scanning microscopes which allow for temporal resolutions up to milliseconds[26] could help to investigate even more complex spatial growth phenomena.

Acknowledgment. We thank R. Magerle for useful discussions and B. Rieger for kindly providing the polymer.

Supporting Information Available: Three avi movie files, M1, SFM phase image sequence of the crystallization process showing an overview of the lamellar evolution, where the total measuring time is 230 min and image size is 1.7 μm $\times$ 2.0 μm, M2, SFM phase image sequence of a growing lamella (boxed area 1 in Figure 1b), where the total measuring time is 230 min and the image size is 240 nm $\times$ 170 nm, and M3, SFM phase image sequence of a growing lamella (boxed area 2 in Figure 1b), where the total measuring time is 230 min, and the image size is 200 nm $\times$ 260 nm. This material is available free of charge via the Internet at http://pubs.acs.org.

References and Notes

(1) Karger-Kocsis, J. *Polypropylene: Structure, blends and composites*, 1st ed.; Chapman & Hall: London, 1995.
(2) Camarillo, A. A.; Stribeck, N. *Fibres Text. Eastern Eur.* **2005**, *13*, 27−29.
(3) Hauser, G.; Schmidtke, J.; Strobl, G.; Thurn-Albrecht, T. *ACS Symp. Ser.* **2000**, *739*, *140*−*151*.
(4) Gradys, A.; Sajkiewicz, P.; Minakov, A. A.; Adamovsky, S.; Schick, C.; Hashimoto, T.; Saijo, K. *Mater. Sci. Eng. A* **2005**, *413*−*414*, 442−446.
(5) Dai, P. S.; Cebe, P.; Capel, M.; Alamo, R. G.; Mandelkern, L. *ACS Symp. Ser.* **2000**, *739*, 152−165.
(6) Zhou, J.; Li, L.; Lu, J. *Polymer* **2006**, *47*, 261−264.
(7) Schönherr, H.; Waymouth, R. M.; Frank, C. W. *Macromolecules* **2003**, *36*, 2412−2418.
(8) Li, L.; Chan, C. M.; Yeung, K. L.; Li, J. X.; Ng, K. M.; Lei, Y. *Macromolecules* **2001**, *34*, 316−325.
(9) McMaster, T. J.; Hobbs, J. K.; Barham, P. J.; Miles, M. J. *Probe Microsc.* **1997**, *1*, 43−56.
(10) Pearce, R.; Vancso, G. J. *Macromolecules* **1997**, *30*, 5843−5848.
(11) Hobbs, J. K.; McMaster, T. J.; Miles, M. J.; Barham, P. J. *Polymer* **1998**, *39*, 2437−2446.
(12) Lei, Y. G.; Chan, C. M.; Li, J. X.; Ng, K. M.; Wang, Y.; Jiang, J.; Li, L. *Macromolecules* **2002**, *35*, 6751−6753.
(13) Zhou, J.; Liu, J. G.; Yan, S. K.; Dong, J. Y.; Li, L.; Chan, C. M.; Schultz, J. M. *Polymer* **2005**, *46*, 4077−4087.
(14) Schönherr, H.; Wiyatno, W.; Pople, J.; Frank, C. W.; Fuller, G. G.; Gast, A. P.; Waymouth, R. M. *Macromolecules* **2002**, *35*, 2654−2666.
(15) Magerle, R. *Phys. Rev. Lett.* **2000**, *85*, 2749−2752.
(16) Rehse, N.; Marr, S.; Scherdel, S.; Magerle, R. *Adv. Mater.* **2005**, *17*, 2203−2206.
(17) Frank, J. *Principles of Electron Tomography*; Plenum: New York, 1992.
(18) Ikehara, T.; Jinnai, H.; Kaneko, T.; Nishioka, H.; Nishi, T. *J. Polym. Sci., Part B: Polym Phys* **2007**, *45*, 1122−1125.
(19) Rieger, B. *J. Am. Chem. Soc.* **1999**, *121*, 4348−4355.
(20) Dietz, C.; Röper, S.; Scherdel, S.; Bernstein, A.; Rehse, N.; Magerle, R. *Rev. Sci. Instrum.* **2007**, *58*, 053703.
(21) Scherdel, S.; Wirtz, S.; Rehse, N.; Magerle, R. *Nanotechnology* **2006**, *17*, 881−887.
(22) Hosier, I. L.; Alamo, R. G.; Lin, J. S. *Polymer* **2004**, *45*, 3441−3445.
(23) Lotz, B.; Graff, S.; Wittmann, J. C. *J. Polym. Sci., Part B: Polym Phys* **1986**, *24*, 2017−2032.
(24) Bassett, D. C. *Philos. Trans. R. Soc. London A* **1994**, *348*, 29−43.
(25) Edwards, B. C.; Phillips, P. J. *Polymer* **1974**, *15*, 351−356.
(26) Hobbs, J. K. *Polymer* **2006**, *47*, 5566−5573.

MA0718649